Proceedings of the 5th International Symposium on Steel Science (ISSS 2017)
Nov. 13-16, 2017, Kyoto, Japan: The Iron and Steel Institute of Japan

Prior austenite grain boundaries in lath martensite: correlation between the crystallographic character and the fracture susceptibility

Fady Archie*, Stefan Zaefferer

Max-Planck-Institut für Eisenforschung, Max-Planck-Str. 1, D-40237 Düsseldorf, Germany

Abstract: Martensite cracks induced by tensile deformation in a ferritic-martensitic DP-steel are characterized in detail using SEM-based electron channelling contrast imaging (ECCI) and EBSD. By reconstruction of the parent austenite grains it is shown that cracks develop particularly along some parts of the prior austenite grain boundaries (PAGBs). Segments of the PAGBs where the adjacent variants keep a Kurdjumov-Sachs orientation relationship with both of the neighbouring parent grains are particularly not fractured. This is attributed to a martensite nucleation mechanism which keeps the local strains and the residual stresses at the PAGB at a low level.

1. INTRODUCTION

Many of the advanced high strength steels incorporate lath martensite (LM) as an essential microstructural component. Although LM elevates the overall strength of the material, it may decline the material formability since deformation-induced crack formation is enhanced within the hard martensitic structure [1]. Recent studies on ferritic-martensitic dual-phase (DP-) steels have shown that the martensite cracks form preferentially along the prior austenite grain boundaries (PAGBs) [2]. One of the possible reasons for the PAGB embrittlement could be the segregation of harmful elements, particularly Mn and P, during the intercritical annealing process [2,3].

The influence of the crystallographic nature of the PAGBs, however, remains unexplored with respect to their susceptibility to intergranular micro-crack formation. The grain boundaries within the parent austenite phase (i.e. the PAGBs) represent the nucleation sites for the martensite variants and it has been shown that along the PAGB, a special variant selection mechanism is induced during the martensitic transformation process [4]. This mechanism entails for a variant nucleating at a γ-γ grain boundary to keep a Kurdjumov-Sachs (K-S) orientation relationship (OR) not only with its parent grain, but also with its neighbouring γ grain (i.e. maintains a double K-S OR) (Fig. 1). Maintaining a double K-S OR minimizes the interface energy between the nucleated variant and each of its neighbouring γ grains, thus enhancing the variant nucleation process [5]. The same mechanism was also demonstrated in upper bainite structures [6]. In this study, we analyse the micro-cracks induced under tensile deformation within the martensitic islands in a DP-steel. We try to reveal whether there is a crystallographic difference between the fractured and the non-fractured segments of the PAGBs, particularly with respect to two parameters, namely, (a) the existence of the double K-S OR, and (b) the misorientation angle measured across the PAGB.

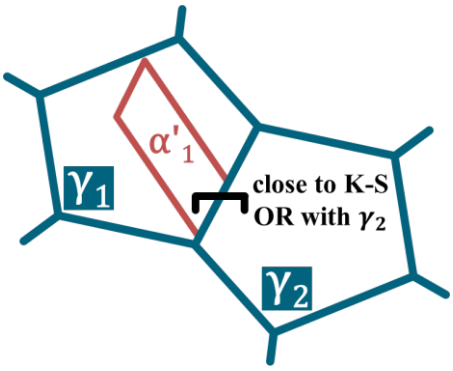

Fig. 1: Schematic illustration of variant nucleation at a γ grain boundary.

2. EXPERIMENTAL

Hot-rolled plain C-Mn steel was utilized, with a chemical composition of Fe-0.14C-1.93Mn-0.42Cr-0.25Si (in wt.%), and an initial bainitic-martensitic phase composition. The microstructure was reaustenitized using a dilatometer DIL 805A/D (TA Instruments) at 840°C for 90 sec., then intercritically annealed for 4 min. at 650°C. The material was finally quenched to room temperature to obtain a DP-steel microstructure. A flat tensile specimen was prepared by spark erosion with a gauge length, width and thickness of 4 mm, 2 mm, and 1 mm, respectively. Monotonic tensile deformation was carried out at an instrument by Kammrath & Weiss GmbH, equipped with a DIC system (ARAMIS, GOM mbH). Deformation was conducted at room temperature up to the onset of

* Corresponding author. E-mail: f.archie@mpie.de, telephone: +49 (0)211 6792 478.

necking at a constant cross-head speed of 5 μm s^{-1}. Four equal-sized areas were selected over the specimen surface for further damage investigation, with average global strain levels of ε_1=0.02, ε_2=0.07, ε_3=0.12, and ε_4=0.16. Around 30 damage features were randomly selected within each area after mechanical silica OPS polishing. The features were captured by secondary electrons (SE) and electron channelling contrast imaging (ECCI), using a Zeiss Merlin SEM, and scanned by EBSD at a step size of 50 nm, using a JEOL JSM-6500F FE-SEM equipped with a TSL OIM system. The damage mechanisms were characterized and categorized according to their common microstructural configurations.

The parent austenite grain structure was reconstructed for the fractured martensitic regions by applying the phase reconstruction algorithm ARPGE to the acquired EBSD data using the Kurdjumov-Sachs (K-S) transformation model at low tolerance angles (< 5°) [7]. For each of the reconstructed parent austenite grains, the ideal orientations of the 24 K-S variants were determined using the Matlab toolbox MTEX in accordance with Table 1.

Variant no.	Invariant plane	Invariant direction	CP group	Bain group	Misorientation from V1 [deg.]
V1	(111)γ//(011)α	[–101]γ//[–1–11]α	CP1	B1	–
V2		[–101]γ//[–11–1]α		B2	60.0
V3		[01–1]γ//[–1–11]α		B3	60.0
V4		[01–1]γ//[–11–1]α		B1	10.5
V5		[1–10]γ//[–1–11]α		B2	60.0
V6		[1–10]γ//[–11–1]α		B3	49.5
V7	(1–11)γ//(011)α	[10–1]γ//[–1–11]α	CP2	B2	49.5
V8		[10–1]γ//[–11–1]α		B1	10.5
V9		[–1–10]γ//[–1–11]α		B3	50.5
V10		[–1–10]γ//[–11–1]α		B2	50.5
V11		[011]γ//[–1–11]α		B1	14.9
V12		[011]γ//[–11–1]α		B3	57.2
V13	(–111)γ//(011)α	[0–11]γ//[–1–11]α	CP3	B1	14.9
V14		[0–11]γ//[–11–1]α		B3	50.5
V15		[–10–1]γ//[–1–11]α		B2	57.2
V16		[–10–1]γ//[–11–1]α		B1	20.6
V17		[110]γ//[–1–11]α		B3	51.7
V18		[110]γ//[–11–1]α		B2	47.1
V19	(11–1)γ//(011)α	[–110]γ//[–1–11]α	CP4	B3	50.5
V20		[–110]γ//[–11–1]α		B2	57.2
V21		[0–1–1]γ//[–1–11]α		B1	20.6
V22		[0–1–1]γ//[–11–1]α		B3	47.1
V23		[101]γ//[–1–11]α		B2	57.2
V24		[101]γ//[–11–1]α		B1	21.1

Table 1: Twenty-four variants in Kurdjumov-Sachs (K-S) orientation relationship.

3. RESULTS AND DISCUSSION

3.1. Characterization of the martensite micro-cracks in DP-steel

Martensite cracks (D_M) constitute more than 60% of the damage features developed within the investigated tensile-deformed DP-steel. Other features mostly resemble damage at the interphase boundaries. A martensite crack is usually located along the narrowest cross-section of a bulk martensite island, and is aligned perpendicular to the tensile loading axis. At low strains (ε_{eng}<7%)

martensite mainly develops partial micro-cracks, i.e. the damaged martensite island is not completely split along the crack direction. By reconstruction of the prior austenite grain structure using ARPGE, more than 90% of the cracks characterized at all strain levels are revealed to form along the PAGBs. Three representative martensite PAGB cracks are illustrated in Fig. 2.

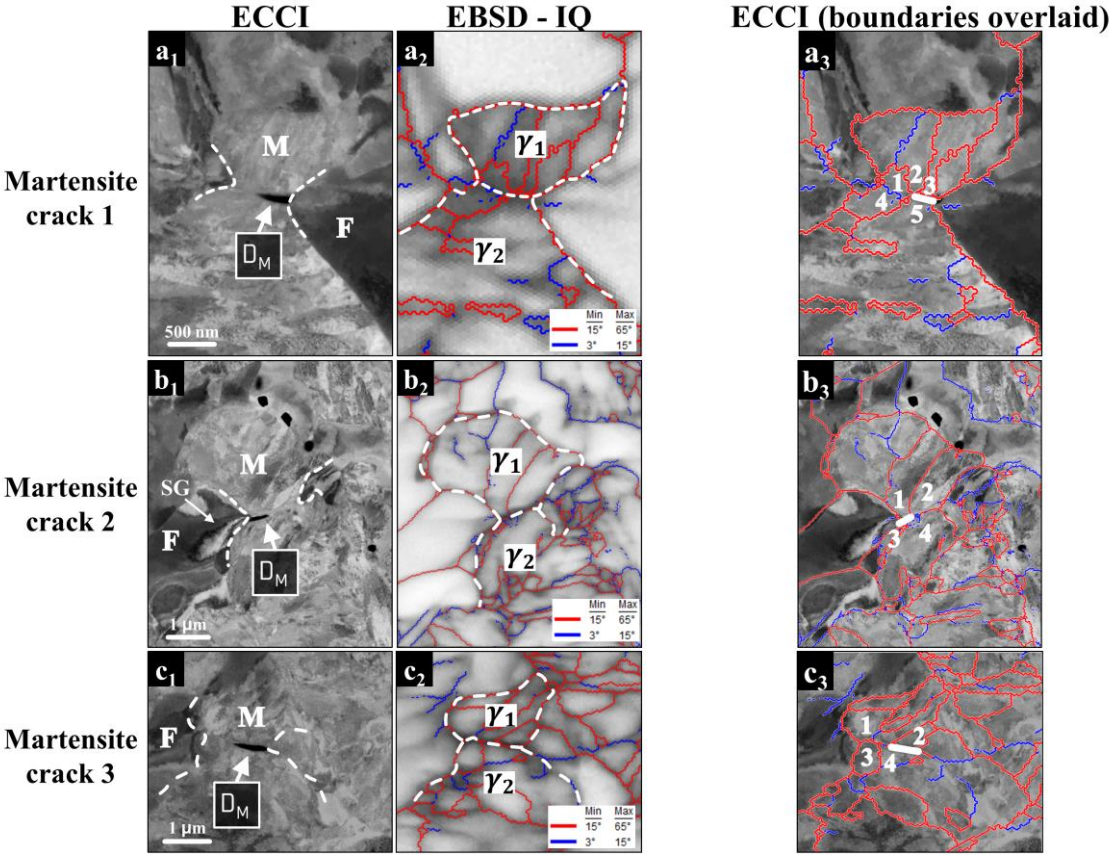

Fig. 2: Three examples of martensitic micro-cracks (D_M) formed along PAGBs in DP-steel. The micro-cracks are illustrated using (a_1-c_1) ECCI images, and (a_2-c_2) corresponding EBSD image quality (-IQ) maps. In (a_3-c_3) the grain boundaries determined by EBSD are superimposed over the ECCI images. The positions of the cracks are manually drawn into (a_3) to (c_3). **M**: martensite, **F**: ferrite, **SG**: orientation gradient.

The parent γ grains are identified using ARPGE reconstruction, and designated as γ_1 and γ_2 for each of the martensite regions in each example (Fig. 2 (a_2) to (c_2)). The lath martensite morphology entails that, within a given parent grain, adjacent laths of similar orientation (within few degrees of misorientation) form a block, whereas a group of adjacent blocks sharing the same invariant plane orientation construct a packet [8]. In Fig. 2 (a_3) to (c_3), the martensite blocks surrounding each of the micro-cracks are given arbitrary numbers to be easily distinguished.

3.2. Relevance of the double K-S OR to the micro-crack formation

For each example, the misorientation angles between the neighbouring martensite blocks across the identified PAGBs were measured (Table 2). Additionally, for each example, Table 2 lists the K-S variant of each of γ_1 and γ_2 grains with minimum misorientation to each of the numbered blocks.

According to Table 2, many of the examined martensite blocks keep low angle misorientations (<15°) to K-S variants of both of the two neighboring parent γ grains (i.e. maintain a double K-S OR). Segments of the PAGBs which obey the double K-S OR are particularly not fractured in the three examples. This applies to PAGB segments between blocks 1 and 4 in example 1, between blocks 2 and 4 in example 2, and finally between blocks 1 and 4 in example 3. Also, cracked segments of the PAGBs often show random high angle grain boundaries while the non-cracked parts more frequently show low-angle grain boundaries or Σ 3 twin boundaries.

From the here presented examples it may be inferred that segments of PAGB where a double K-S OR prevails might be more resistant to fracture that others. If a variant (α'_1) nucleates at a γ_1-γ_2

boundary while maintaining a K-S OR with both γ grains (Fig. 1), minimum strains are induced in the vicinity of the γ-γ boundary. This is based on experimental evidence of Miyamoto et al. [9], who did not observe any lattice distortions within the neighbouring parent grain, given that a martensite lath with double K-S OR developed in one austenite grain. Therefore, segments of PAGBs with double K-S OR may not only show low interface energy, but are also expected to be surrounded by less severe transformation-induced strain localizations. Both factors may enhance the plastic deformability of those particular segments, thus improving their fracture toughness. The existence of low angle and Σ3 boundaries could be correlated to the double K-S OR, as similarly presumed for upper bainite [6].

	Double K-S OR analysis						**Misorientation and condition of the boundary**		
	Parent grain no.	Block no.	Misorientation to closest γ_1 K-S variant		Misorientation to closest γ_2 K-S variant		Misorientation between martensite blocks across PAGB		Condition of the boundary
			Misorient. angle [deg.]	Variant no.	Misorient. Angle [deg.]	Variant no.	Segment (block no.)	Misorient. angle [deg.]	
Martensite crack 1	γ_1	**1**	5	V5	1	V6	**1 – 4**	12	undamaged
		2	5	V9	22	V8	**2 – 5**	42	crack
		3	4	V11	22	V16	**3 – 5**	48	crack
	γ_2	**4**	10	V10	7	V19			
		5	27	V8	3	V1			
Martensite crack 2	γ_1	**1**	3	V9	11	V10	**1 – 3**	39	crack
		2	3	V10	14	V9	**1 – 4**	52 (Σ3)	crack
	γ_2	**3**	20	V8	9	V13	**2 – 4**	13	undamaged
		4	7	V23	4	V9			
Martensite crack 3	γ_1	**1**	3	V13	6	V11	**1 – 3**	53 (Σ3)	undamaged
		2	8	V17	25	V17	**1 – 4**	14	undamaged
	γ_2	**3**	18	V22	4	V12	**2 – 4**	56	crack
		4	7	V4	2	V11			

Table 2: Analysis results of the martensitic micro-cracks in Fig. 2.

4. CONCLUSIONS

Martensite variants adjacent to the prior austenite grain boundaries (PAGBs) frequently maintain a K-S orientation relationship with both of their neighbouring parent grains. This mechanism is known as double K-S OR. In DP-steels, martensite cracks develop along PAGBs, however, segments with double K-S OR are usually not fractured. The double K-S OR is suggested to enhance the fracture strength of the boundary by reducing both the interface energy and the transformation-induced localized strain concentrations.

5. REFERENCES

[1] C. C. Tasan, M. Diehl, D. Yan, M. Bechtold, F. Roters, L. Schemmann, C. Zheng, N. Peranio, D. Ponge, M. Koyama, K. Tsuzaki and D. Raabe: Annual Reviews of Materials Research, 45 (2015), 391-431.
[2] F. Archie, X. Li and S. Zaefferer: Materials Science and Engineering A, 701 (2017), 302-313.
[3] M. Kuzmina, D. Ponge and D. Raabe: Acta Materialia, 86 (2015), 182-192.
[4] S. Morito, J. Nishikawa, T. Ohba, T. Furuhara and T. Maki: in International Conference on Martensitic Transformations (ICOMAT), Santa Fe, New Mexico, 2008.
[5] D. W. Kim, D.-W. Suh, R. S. Qin and H. K. D. H. Bhadeshia: Journal of Materials Science, 45 (2010), 4126-4132.
[6] T. Furuhara, H. Kawata, S. Morito, G. Miyamoto and T. Maki: Metallurgical and Materials Transactions A, 39 (2008), 1003-1013.
[7] C. Cayron: Applied Crystallography, 40 (2007), 1183-1188.
[8] S. Morito, H. Tanaka, R. Konishi, T. Furuhara and T. Maki: Acta Materialia, 51 (2003), 1789-1799.
[9] G. Miyamoto, A. Shibata, T. Maki and T. Furuhara: Acta Materialia, 57 (2009), 1120-1131.